Necklacelike Solitons in Optically Induced Photonic Lattices

Article *in* Physical Review Letters · April 2005

DOI: 10.1103/PhysRevLett.94.113902 · Source: PubMed

7 authors, including:

Igor Makasyuk
Stanford University
45 PUBLICATIONS **1,607** CITATIONS

SEE PROFILE

D. J. Frantzeskakis
National and Kapodistrian University of Athens
364 PUBLICATIONS **9,018** CITATIONS

SEE PROFILE

Zhigang Chen
San Francisco State University
496 PUBLICATIONS **10,865** CITATIONS

SEE PROFILE

Necklacelike Solitons in Optically Induced Photonic Lattices

J. Yang,[1] I. Makasyuk,[2] P. G. Kevrekidis,[3] H. Martin,[2] B. A. Malomed,[4] D. J. Frantzeskakis,[5] and Zhigang Chen[2,6]

[1]*Department of Mathematics and Statistics, University of Vermont, Burlington, Vermont 05401, USA*
[2]*Department of Physics and Astronomy, San Francisco State University, San Francisco, California 94132, USA*
[3]*Department of Mathematics and Statistics, University of Massachusetts, Amherst, Massachusetts 01003, USA*
[4]*Department of Interdisciplinary Studies, Faculty of Engineering, Tel Aviv University, Tel Aviv 69978, Israel*
[5]*Department of Physics, University of Athens, Panepistimiopolis, Zografos, Athens 15784, Greece*
[6]*TEDA College, Nankai University, Tianjin, China*

(Received 30 September 2004; published 22 March 2005)

We report the first observation of stationary necklacelike solitons. Such necklace structures were realized when a high-order vortex beam was launched appropriately into a two-dimensional optically induced photonic lattice. Our theoretical results obtained with continuous and discrete models show that the necklace solitons resulting from a charge-4 vortex have a π phase difference between adjacent ''pearls'' and are formed in an octagon shape. Their stability region is identified.

DOI: 10.1103/PhysRevLett.94.113902 PACS numbers: 42.65.Tg

A necklace beam is a ring-shaped beam with a periodic intensity change along the azimuthal direction. Since the effective radius of the ring is much larger than its thickness, the intensity spots within the ring look like pearls in a necklace. It has been found that such a beam can exhibit self-trapping in a focusing Kerr medium [1], although it is well-known that in general $(2 + 1)$-dimensional [$(2 + 1)$D] solitons in such a medium are inherently unstable [2]. For a necklace beam, it is the interaction between ''pearls'' that stabilizes the structure as a whole, while each pearl alone cannot form a stable soliton [3]. Importantly, a self-trapped necklace-ring beam represents a soliton cluster in nonlinear optics, which can carry zero or nonzero angular momentum [3–5], and this type of soliton structure may also exist in other nonlinear systems [including Bose-Einstein condensates (BECs) trapped in a two-dimensional optical lattice [6]]. However, the self-trapped necklace beams found thus far are not stationary soliton configurations in a strict sense, as they either gradually expand in the radial direction [1] or rotate in the angular direction [3,4]. A similar object is the necklace pattern of vortex pairs predicted theoretically in a 2D BEC model [7]. Other types of 2D soliton complexes have also been found recently in various continuum [8] and discrete [9] systems. In spite of all these theoretical studies, the experimental observation of necklacelike soliton propagation remains a challenge.

Recently, there has been increasing interest in the study of solitons and localized states in nonlinear periodic systems [10]. The collective behavior of wave propagation in a periodic structure exhibits many intriguing phenomena that cannot be found in homogeneous media (such as discrete diffraction, Peierls barriers, and lattice vortices [10]). When a waveguide array is embedded in a nonlinear medium, a balance between discrete diffraction and nonlinear self-focusing leads to the formation of lattice solitons [10–14]. During the last few years, lattice solitons have been demonstrated in fabricated AlGaAs waveguide arrays [11] and in optically induced photorefractive (PR) waveguide lattices [12–14]. In addition, lattice vortex solitons [15,16], lattice dipole solitons [17], and lattice soliton trains [18] have been successfully observed experimentally in 2D photonic lattices created by optical induction. Such soliton structures cannot exist with self-focusing nonlinearity should the lattice potential be removed. Thus, it is natural to inquire whether more complicated bound states such as necklace-shaped solitons can be observed in a 2D photonic lattice.

In this Letter, we report the first observation of stationary necklacelike solitons. Such necklace structures are generated by launching a vortex beam with a topological charge $m = 4$ into a 2D square lattice created in a PR crystal with partially coherent light. Inspired by the recent theoretical work on vortex solitons in lattices [19–21], we corroborate the experimental results by detailed computations in theoretical models. Our theoretical results obtained from a continuous model with a periodic lattice potential as well as a relevant discrete model indicate that such necklace solitons with an octagon shape and π phase difference between adjacent pearls exist and are stable under certain conditions—in good agreement with the experimental observations. These results may pave the way for observation of similar phenomena in other discrete or periodic nonlinear systems.

Our experiments were performed in a 2D square lattice optically induced by passing a laser beam (with wavelength $\lambda = 488$ nm) through a rotating diffuser, an amplitude mask, and a biased PR crystal, as introduced in Ref. [22]. The amplitude mask provides periodic spatial modulation on the beam after the diffuser and thus results in a partially coherent lattice beam. The biased crystal (20 mm long SBN:60) provides a self-focusing noninstantaneous nonlinearity. Because of the anisotropic property of the PR crystal, the ordinarily polarized lattice beam experiences only a weak nonlinearity and forms a stable 2D waveguide array nearly invariant during propagation in

the crystal, as first proposed in Ref. [23]. The principal axes of the square lattice are oriented in the diagonal directions. To facilitate the formation of a necklacelike soliton, a ring vortex beam is launched into the lattice such that the ring covers 8 lattice sites, with the center of the ring located in an empty site (off site) as shown in Fig. 1(a). The ring vortex is created with a charge-4 helicoidal phase mask, and the phase singularity of the vortex is shown in the interferograms of Figs. 1(b) and 1(c). The vortex beam is coherent (without going through the diffuser) and extraordinarily polarized. Thus, it experiences a much higher nonlinearity while propagating collinearly with the lattice beam through the biased crystal [14]. In addition, a uniform incoherent beam is used as background illumination for fine-tuning the nonlinearity.

Typical experimental results of the high-order vortex propagation with and without the 2D optically induced lattice are presented in Fig. 2, where a stable square lattice (with 40 μm lattice spacing) is first created in the crystal. A vortex beam with charge-4 and intensity about 5 times weaker than that of the lattice is then launched into the lattice, with the vortex ring covering 8 sites in a necklace or octagon shape as shown in Fig. 1(a). The vortex beam at the crystal input is shown in Fig. 2(a), and it exhibits significant diffraction after linear propagation through a 20 mm long crystal [Fig. 2(b)]. Without the lattice, the charge-4 vortex breaks up into many filaments in the self-focusing nonlinear crystal, leading to disordered patterns driven by noise and modulation instability [24]. Figures 2(c) and 2(d) show two such output patterns at different levels of nonlinearity as controlled by the bias field. In the presence of the lattice, however, the behavior of the vortex is dramatically different, characterized by the confinement of the filaments at about the location of the initial vortex ring. This is shown in the bottom panel of Fig. 2, where the vortex beam exhibits discrete diffraction when the nonlinearity is low [Fig. 2(e)] but evolves into a necklacelike structure at an appropriate level of high nonlinearity [Fig. 2(f)]. Such a soliton cluster is stationary and quite stable during the period of observation (typically more than 30 min), so the soliton structure is observed in steady state. Furthermore, following the procedure in Refs. [14,15], it is concluded that the observed self-trapping is due to the nonlinear self-action of the vortex-ring beam, as the waveguide lattice is nearly the same in Figs. 2(e) and 2(f). When the center of the initial vortex ring is moved from the off-site position to an on-site one, the octagon structure disappears [Fig. 2(g)]. But when the vortex ring is lined up again with 8 octagon-shaped lattice sites (at a different off-site location), the necklace structure is restored in a new steady state [Fig. 2(h)]. Thus the off-site excitation favors the formation of the necklace soliton, possibly due to that in such a configuration the circular symmetry of the necklace beam can be maintained in the lattice. The experiment was repeated with vortices of different topological charges. When a ring vortex beam with charge lower than 4 is launched into the same octagon-shaped lattice sites, less confined necklace structures are observed. Even for the case of a charge-4 vortex where the robust necklace structure is observed, we could not achieve sufficiently high visibility to determine the entire phase structure of the necklace soliton by the interference technique, as was done for charge-1 lattice vortex solitons [15,16]. This is simply due to the imperfection of the vortex mask that results in unequal intensities for the pearls in the necklace and the strong sensitivity to the background noise.

The above experimental results are corroborated by our theoretical results obtained by means of two different (yet complementary) approaches. First, we use a continuous model with a periodic lattice potential that describes the underlying PR crystal [12,20]:

$$iU_z + U_{xx} + U_{yy} - \frac{E_0}{1 + I_l + |U|^2} U = 0, \qquad (1)$$

where U is the slowly varying amplitude of the probe beam normalized by the dark irradiance of the crystal I_d, and $I_l = I_0 \sin^2\{(x + y)/\sqrt{2}\} \sin^2\{(x - y)/\sqrt{2}\}$ is a square-

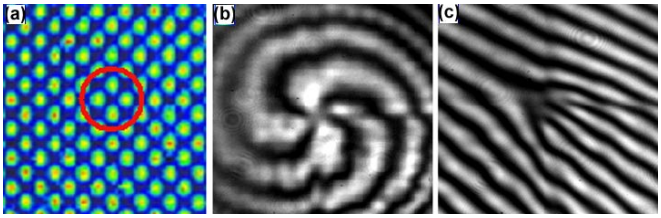

FIG. 1 (color online). Left: a 2D photonic lattice (40 μm spacing) created by optical induction, where the circle indicates the off-site vortex location. Middle and right: interferograms of a charge-4 vortex with a spherical and a plane wave, respectively.

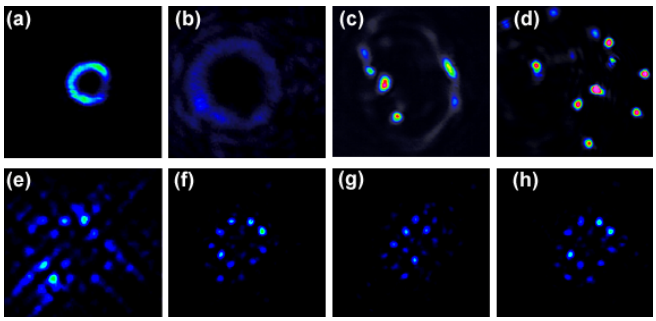

FIG. 2 (color online). Experimental results of charge-4 vortex propagating without (top) and with (bottom) the 2D lattice. (a) input, (b) linear diffraction, (c) output at a bias field of 90 V/mm, (d) output at 240 V/mm, (e) discrete diffraction at 90 V/mm, (f)–(h) discrete trapping at 240 V/mm. From (f) to (h), the vortex was launched from off-site, to on-site, and then back to off-site configurations. Distance of propagation through the crystal: 20 mm; average distance between adjacent pearls in the necklace: 48 μm.

lattice intensity function (in units of I_d) which closely resembles the lattice created in our experiment. Here I_0 is the lattice peak intensity, z is the propagation distance (in units of $2k_1D^2/\pi^2$), (x, y) are transverse coordinates (in units of D/π), E_0 is the applied dc field [in units of $\pi^2/(k_0^2 n_e^4 D^2 r_{33})$], D is the lattice spacing, $k_0 = 2\pi/\lambda_0$ (λ_0 is the wavelength), $k_1 = k_0 n_e$, n_e is the unperturbed refractive index, and r_{33} is the electro-optic coefficient of the crystal for the extraordinarily polarized light beam. Consistent with our experiment, we choose the lattice intensity $I_0 = 3I_d$. In addition, we choose other physical parameters as $D = 20$ μm, $\lambda_0 = 0.5$ μm, $n_e = 2.3$, and $r_{33} = 280$ pm/V. Thus, in these computations, one unit of x or y corresponds to 6.4 μm, one unit of z corresponds to 2.3 mm, and one unit of E_0 corresponds to 20 V/mm.

Necklace solitons in the shape of octagons in Eq. (1) are sought in the form of $U = u(x, y)e^{-i\mu z}$, where u is a real-valued function, and μ is the propagation constant. The solution u can be determined by an iteration method (see [25] for a detailed description of this method). These solitons have 8 pearls forming an octagon-shaped structure inside the lattice-induced waveguides, and adjacent pearls have π phase difference. Such a necklace soliton at $E_0 = 6.5$, $I_0 = 3$, and $\mu = 3$ is shown in Fig. 3(b), and the corresponding lattice pattern is shown in Fig. 3(a). One can view this necklace soliton as a few diagonal and nondiagonal dipole solitons pieced together [17]. The peak intensity diagram of these necklace solitons versus the propagation constant μ is displayed in Fig. 3(c). This peak intensity is a decreasing function of μ. The power (not shown) is a decreasing function of μ as well. Below a critical value of μ, which is about 2.1 at $E_0 = 6.5$ and $I_0 = 3$, this family of necklace solitons disappears. We have determined the linear stability properties of these solitons as well, and their leading unstable eigenvalues versus μ are shown in Fig. 3(d). We see that these solitons are stable when μ falls within a certain interval (μ_1, μ_2), or equivalently, when their peak intensities I fall within a corresponding interval (I_1, I_2), but are unstable otherwise. At $E_0 = 6.5$ and $I_0 = 3$, $\mu_1 \approx 2.74$, $\mu_2 \approx 3.31$, or equivalently, $I_1 = 3.69$, $I_2 = 7.43$ [see Fig. 3(d)]. As the voltage E_0 increases, necklace solitons get more stabilized. These behaviors are similar to those of dipole and vortex solitons reported before [17,20].

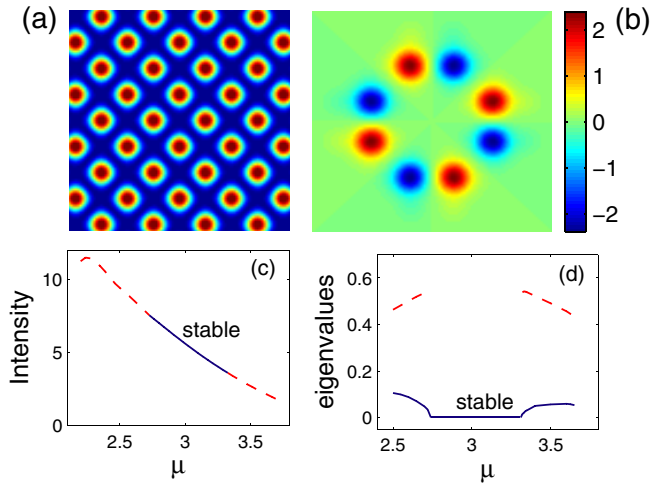

FIG. 3 (color online). (a) Lattice intensity pattern; (b) field $u(x, y)$ of a necklace soliton with peak intensity $5I_d$; side bar: color map of the field; (c) intensity diagram; dashed parts indicate unstable solitons; (d) leading unstable eigenvalues σ versus μ; solid line: Re(σ); dashed line: Im(σ). Here $E_0 = 6.5$ and $I_0 = 3$.

In the experiments reported above, we launched a ring vortex with charge-4 into a crystal. This input has an angular momentum, but the theoretically obtained necklace solitons in Fig. 3 do not. Thus the question arises whether or not a vortex with an angular momentum can evolve into a necklace soliton with no angular momentum upon certain distance of propagation. However, in the presence of the photonic lattice, the angular momentum is not preserved; thus such evolution is clearly possible. To study this evolution theoretically, we simulated Eq. (1) starting from a ring vortex with charge-4. The input conditions and physical parameters used in our simulations resemble those in our experiments. Specifically, the center of this ring is set off site, its radius is 1.6 times the lattice spacing, and its peak intensity is 1/6 that of the lattice. The background illumination is about 1/3 of the lattice's peak intensity. The lattice spacing is 20 μm, and the simulation distance is 20 mm. The simulation results at low (40 V/mm) and high (300 V/mm) applied fields are shown in Fig. 4. At low applied fields where the nonlinearity is weak, the vortex experiences discrete diffraction and splits into four fragments [see Fig. 4(b)], analogous to the experimental result [see Fig. 2(e)]. At high applied fields, however, the vortex does evolve into a necklacelike structure [Fig. 4(c)]. Examination of the phase field [Fig. 4(d)] confirms that the eight pearls in the necklace are indeed π out of phase, indicating that this is a true necklace soliton with no angular momentum. We have continued the simulation to much longer distances, and found that this necklace structure is very robust, in agreement with the linear stability results shown in Fig. 3(d). With a charge-1 vortex launched at the same conditions,

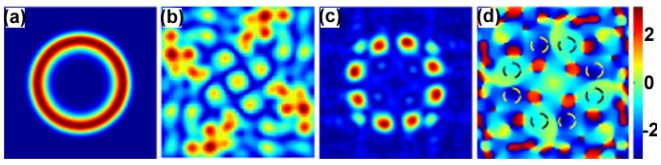

FIG. 4 (color online). Theoretical results for an initial ring vortex with charge-4 after 20 mm propagation. (a) input; (b),(c) intensity plots at low (40 V/mm) and high ($V =$ 300 V/mm) applied fields; (d) phase plot of (c). The dashed lines in (d) correspond to the positions of the eight intensity lobes. Side bar: phase color map. The lattice is as in Fig. 3(a).

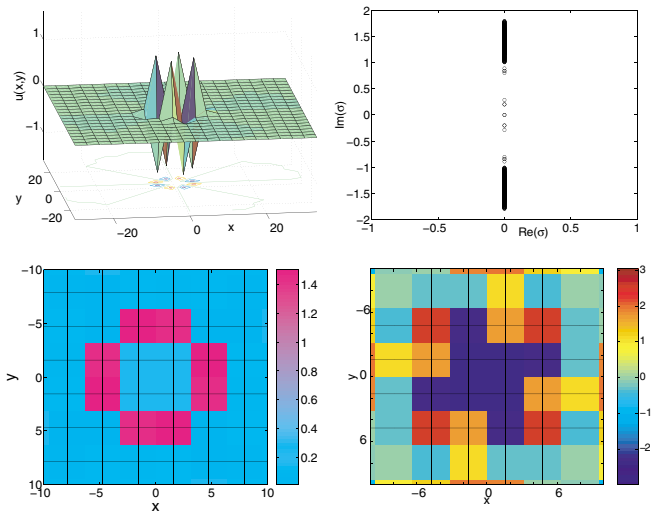

FIG. 5 (color online). Top left: the (stable) discrete octagon profile for $C = 0.1$. Top right: linearization spectrum of this octagon. The absence of eigenvalues with $\mathrm{Re}(\sigma) > 0$ indicates stability. Bottom panel: amplitude and phase of the initial charge-4 vortex at $z \approx 500$, $C = 0.1$.

we have found numerically that it does not evolve into a stable necklace structure.

We now turn to a relevant discrete nonlinear model to which nonlinear Schrödinger equations with a periodic potential can be reduced [26]. This model is the discrete nonlinear Schrödinger equation of the form

$$i\frac{\partial U_{m,n}}{\partial z} = C\Delta_2 U_{m,n} + |U_{m,n}|^2 U_{m,n,}, \qquad (2)$$

where $\Delta_2 U_{m,n}$ is the 2D discrete Laplacian, and C is the intersite linear coupling coefficient. Substituting $U(m, n, z) = u_{m,n}e^{-i\mu z}$, we solved the steady state equation for the profile u by means of an iterative method. We then performed full linear stability analysis, using the linearization $\phi_{m,n} = e^{-i\mu z}\{u_{m,n} + \epsilon[a_{m,n}e^{\sigma z} + b_{m,n}e^{\sigma^* z}]\}$, where ϵ is an infinitesimal amplitude of the perturbation, and σ is its eigenvalue. The resulting eigenvalue problem for $\{\sigma, [a, b^*]^T\}$ is subsequently solved to determine the linear stability of the solution. Since varying μ and C is equivalent (modulo a rescaling), we fix $\mu = 1$ and vary the intersite coupling C. In the anticontinuum limit [10] of $C = 0$, an octagon configuration can be straightforwardly constructed. Such solutions persist for $C > 0$. Regarding their linear stability, we have found that below a critical coupling of $C_{\mathrm{cr}} = 0.106$, these necklace solutions are indeed linearly stable (an example is shown in Fig. 5 for $C = 0.1$). But for stronger coupling of $C > C_{\mathrm{cr}}$, it may become unstable with up to seven eigenvalue quartets [27]. Typical simulation results using the discrete model for evolution of a charge-4 ring-beam into an octagon structure at $C < C_{\mathrm{cr}}$ is shown in Fig. 5 (bottom). These results are consistent with those from the continuous model, as the intersite overlap (coupling) of necklace solitons in the continuous model (1) becomes large when their peak intensities are either very low or very high.

In summary, we have demonstrated both experimentally and theoretically the existence, stability, and robustness of necklace solitons in an optically induced photonic lattice. Our results may be relevant to other periodic nonlinear systems in optical, atomic, and condensed-matter physics.

This work was supported by AFOSR, ARO, NASA EPSCoR, NSFC, NSF, ISF, and Eppley. We are indebted to P. Maker, R. Muller, and D. Wilson for fabricating the high-order vortex mask.

[1] M. Soljacic *et al.*, Phys. Rev. Lett. **81**, 4851 (1998).
[2] P. L. Kelley, Phys. Rev. Lett. **15**, 1005 (1965).
[3] M. Soljacic and M. Segev, Phys. Rev. E **62**, 2810 (2000); Phys. Rev. Lett. **86**, 420 (2001).
[4] A. S. Desyatnikov and Yu. S. Kivshar, Phys. Rev. Lett. **87**, 033901 (2001); **88**, 053901 (2002).
[5] Y. V. Kartashov *et al.*, Phys. Rev. Lett. **89**, 273902 (2002).
[6] S. Burger *et al.*, Europhys. Lett. **57**, 1 (2002).
[7] G. Theocharis *et al.*, Phys. Rev. Lett. **90**, 120403 (2003).
[8] Y. V. Kartashov *et al.*, Opt. Lett. **29**, 1918 (2004).
[9] P. G. Kevrekidis *et al.*, J. Phys. A **34**, 9615 (2001).
[10] D. N. Christodoulides *et al.*, Nature (London) **424**, 817 (2003); P. G. Kevrekidis *et al.*, Int. J. Mod. Phys. B **15**, 2833 (2001).
[11] H. S. Eisenberg *et al.*, Phys. Rev. Lett. **81**, 3383 (1998).
[12] J. W. Fleischer *et al.*, Nature (London) **422**, 147 (2003).
[13] D. Neshev *et al.*, Opt. Lett. **28**, 710 (2003).
[14] H. Martin *et al.*, Phys. Rev. Lett. **92**, 123902 (2004).
[15] D. N. Neshev *et al.*, Phys. Rev. Lett. **92**, 123903 (2004).
[16] J. W. Fleischer *et al.*, Phys. Rev. Lett. **92**, 123904 (2004).
[17] J. Yang *et al.*, Opt. Lett. **29**, 1662 (2004).
[18] Z. Chen *et al.*, Phys. Rev. Lett. **92**, 143902 (2004).
[19] B. A. Malomed and P. G. Kevrekidis, Phys. Rev. E **64**, 026601 (2001).
[20] J. Yang and Z. H. Musslimani, Opt. Lett. **28**, 2094 (2003); B. B. Baizakov *et al.*, Europhys. Lett. **63**, 642 (2003).
[21] P. G. Kevrekidis *et al.*, Phys. Rev. E **70**, 056612 (2004).
[22] Z. Chen and K. McCarthy, Opt. Lett. **27**, 2019 (2002).
[23] N. K. Efremidis *et al.*, Phys. Rev. E **66**, 046602 (2002).
[24] W. J. Firth and D. V. Skryabin, Phys. Rev. Lett. **79**, 2450 (1997).
[25] J. Yang *et al.*, Stud. Appl. Math. **113**, 389 (2004).
[26] G. L. Alfimov *et al.*, Phys. Rev. E **66**, 046608 (2002).
[27] D. E. Pelinovsky *et al.*, nlin.PS/0411016.